Cell Cycle Arrest Induced by Hydrogen Peroxide Is Associated with Modulation of Oxidative Stress Related Genes in Breast Cancer Cells

PEI-JOU CHUA, GEORGE WAI-CHEONG YIP, AND BOON-HUAT BAY[1]

Department of Anatomy, Yong Loo Lin School of Medicine, National University of Singapore, Singapore 117 597, Singapore

Depending on the amounts present, reactive oxygen species can exert either beneficial or deleterious effect to cells. In the present study, we observed a decrease in cell viability concomitant with an increase of malondialdehyde concentration in hydrogen peroxide (H_2O_2)-treated MCF-7 breast cancer cells. There was also a concurrent G1/S phase cell cycle arrest with increased apoptosis in H_2O_2-treated cells. Analysis of 84 oxidative stress related genes showed that five genes were significantly and differentially regulated, namely, *Cytoglobin (CYGB), Forkhead box M1 (FOXM1), NADPH oxidase* (*NOX5), Nudix (nucleoside diphosphate linked moiety X)-type motif 1 (NUDT1)* and *Selenoprotein P1 (SEPP1)* genes with H_2O_2 treatment. It would seem that oxidative stress induces cell cycle arrest in the breast cancer by modulation of these genes. Manipulation of these genes, in particular *FOXM1*, a proliferation-specific gene associated with human malignancies, could stifle cancer progression and enhance the therapeutic efficacy of drugs which exert their effects by oxidative stress. Exp Biol Med 234:1086–1094, 2009

Key words: hydrogen peroxide; oxidative stress; cell cycle; Forkhead box M1 (FOXM1); breast carcinoma

Introduction

Reactive oxygen species (ROS) such as superoxide anions (O_2^-), hydroxyl radicals (OH), and hydrogen peroxides (H_2O_2) can lead to oxidative damage resulting in impairment of protein function, mutation of nucleic acids and lipid peroxidation (1, 2). ROS has been implicated in aging (3), as well as development of diseases such as Alzheimer's disease (4), Parkinson's disease (5) and atherosclerosis (6). Moreover, there are reports that oxidative stress contributes to oncogenic development via induction of DNA damage that lead to mutation and increased cell proliferation, survival and migration (7).

Studies have shown that at lower concentrations in mammalian cells, ROS may serve as secondary messengers by activating signal transduction pathways mediated by tyrosine kinases, mitogen-activated protein kinases, protein kinase C, epidermal growth factor receptor, protein phosphatases, potassium channels, activator protein-1 and nuclear factor κB (8). As H_2O_2 is a small and uncharged molecule, its ability to diffuse freely across plasma membranes, makes it an ideal candidate as a signaling molecule (9). However, in the presence of iron, H_2O_2 can be converted into a hydroxyl radical, which can oxidize molecular targets before conversion to water by enzymatic or non-enzymatic antioxidants (10). Overproduction of ROS and deficiency in antioxidant enzymes could lead to cytotoxicity by damaging cell components (11, 12). Therefore, it would seem that ROS can have dual roles, either beneficial or deleterious, depending on the levels in living cells.

The study of cellular responses to ROS could provide an understanding of the mechanism and pathogenesis of diseases related to oxidative stress and provides insights into anti-oxidant defense against oxidative stress. The objective of the present study was to investigate the effects of oxidative stress mediated by H_2O_2 on cell viability and cell cycle profile and determine the changes in expression of oxidative stress related genes in MCF-7 breast cancer cells. The results presented here demonstrate that hydrogen peroxide induced cell cycle arrest and modulation of oxidative stress related genes.

Materials and Methods

Materials. Cell culture reagents were procured from Life Technologies Inc. (Rockville, MD) and fetal bovine

This work was supported by Singapore National Medical Research Council Grant NMRC/1081/2006.

[1] To whom correspondence should be addressed at Department of Anatomy, Yong Loo Lin School of Medicine, National University of Singapore, 4 Medical Drive, Blk MD10, Singapore 117 597, Singapore. E-mail: antbaybh@nus.edu.sg

Received March 5, 2009.
Accepted May 18, 2009.

DOI: 10.3181/0903-RM-98
1535-3702/09/2349-1086$15.00

serum (FBS) was purchased from Hyclone Laboratories (Logan, UT). H_2O_2 solution was obtained from Kanto Chemical (Tokyo, Japan).

Cell Culture. The MCF-7 breast cancer cell line (HTB-22) was obtained from the American Type Culture Collection (Rockville, MD) and was grown in Dulbecco's modified Eagles medium (DMEM) containing 10% FBS at 37°C in a 5% CO_2 incubator.

H_2O_2 Treatment. A 34.5% w/v H_2O_2 stock solution was dissolved with DMEM to make a 25 mM H_2O_2 solution. Different concentrations of H_2O_2 were then prepared, stored at 4°C and used within 24 hours after thawing.

Cell Viability Assay. Cell viability was determined by a 3-(4,5-dimethylthiazol-2-yl)-5-(3-carboxymethoxyphenyl)-2-(4-sulfophenyl)-2H-tetrazolium (MTS) assay using the commercially available CellTiter 96® AQueous Non-Radioactive Cell Proliferation Assay (Promega, Madison, WI). MCF-7 breast cancer cells were cultured in a 96-well plate with 1×10^4 cell density and treated with H_2O_2 for 24 hours before performing the MTS assay.

Confocal Microscopy. Cells were grown on cover slips and were treated with H_2O_2 for 24 hours before fixing with 4% formaldehyde for 15 minutes. Cells were stained with 4,6-diamidino-2-phenylindole (DAPI) fluorochrome dye (Santa Cruz Biotechnology, Inc., Santa Cruz, CA) and observed under an Olympus Fluoview™ confocal microscope (Tokyo, Japan).

Cell Cycle Analysis. Cells were trypsinized, collected by centrifugation and washed twice with PBS. Cell pellets were resuspended in 0.5 ml PBS and fixed in 4.5 ml 70% cold ethanol overnight at 4°C. Ethanol-fixed cells were centrifuged at 1800 rpm for 5 minutes and washed with PBS twice to remove ethanol. One ml of cocktail solution (8 ml of PBS, 10 µl of Triton-X, 2 ml of RNAse A 1 mg/ml, and 200 µl of propidium iodide 1 mg/ml) was added to the cell pellet and incubated for 30 minutes at room temperature before analysis by flow cytometry.

Lipid Peroxide Assay. Cell suspensions were centrifuged at 1000 rpm for 5 minutes and washed twice with Phosphate Buffered Saline (PBS). Supernatants were discarded and cell pellets resuspended in 1 ml PBS and sonicated using ultrasonic processor three times for 5-second intervals at 40 V setting over ice. Lipid peroxidation was determined by the measurement of thiobarbituric acid reactive substances (TBARS) using the TBARS assay kit (Cayman Chemical, Ann Arbor, MI), according to the manufacturer's protocol.

RNA Isolation. Total RNA was isolated from MCF-7 cells using the RNeasy Mini Kit (Qiagen, Valencia, CA). The quantity and quality of the RNA extracts were determined by measuring the absorbance at 260 nm and 280 nm using a NanoDrop® ND-1000 Spectrophotometer (Thermo Scientific Inc., Waltham, MA).

Oxidative Stress and Antioxidant Defense PCR Microarray. Each RNA sample (0.5 µg) was mixed with 2 µl of 5× Genomic DNA Elimination Buffer and made up to a final volume of 10 µl. The mixture content was then incubated at 42°C for 5 minutes and chilled on ice for at least 1 minute. 10 µl of RT cocktail (prepared according to the manufacturer's instruction) was added to 10 µl Genomic DNA Elimination Mixture and incubated at 42°C for 15 minutes, followed by heating at 95°C for 5 minutes. 91 µl of ddH_2O was added to each 20 µl of cDNA Synthesis Reaction. Real-time PCR was performed using the Human Oxidative Stress and Antioxidant Defense RT^2 Profiler PCR microarray according to the manufacturer's protocol (SuperArray Bioscience, Frederick, MD). Gene expression was compared according to the C_T value. The normalizer used for each cDNA sample was the average of five housekeeping genes, *viz., Hypoxanthine phosphoribosyltransferase 1, Beta-2-microglobulin, Ribosomal protein L13a, Glyceraldehyde-3-phosphate dehydrogenase* and *beta actin.*

Quantitative RT-PCR. 0.5 µg of total RNA was reverse transcribed using SuperScript III first strand cDNA synthesis kit (Invitrogen, Carlsbad, CA) with random hexamer according to manufacturer's instruction. The cDNA was used as a template for real time quantitative PCR analysis using the LightCycler technique (Roche Diagnostics GmbH, Mannheim, Germany). The PCR reaction mixture consisted of QuantiTect SYBR Green PCR master mix (2× QuantiTect SYBR Green kit, contains HotStart Taq® DNA polymerase, QuantiTect SYGB Green PCR buffer, dNTP mix, SYGB I, Rox passive reference dye and 5 mM $MgCl_2$) (Qiagen, Valencia, CA), 0.5 µmol/L of each primer and cDNA. The transcripts of the housekeeping gene, *Glyceraldehyde-3-phosphate dehydrogenase (G3PDH)* and transcription factor *Forkhead box M1 (FOXM1)* were detected by the following pair of primers: 5′-GAA GGT GAA GGT CGG AGT CAA CG-3′ (forward) and 5′-TGC CAT GGG TGG AAT CAT ATT GG-3′ (reverse); and 5′-AAC CGC TAC TTG ACA TTG G-3′ (forward) and 5′-GCA GTG GCT TCA TCT TCC-3′ (reverse), respectively.

Western Blot Analysis. Cells were lysed with lysis buffer containing 7 M urea, 2 M thiourea, 4% CHAPS, 20 mM Tris, 1× nuclease mix and protease inhibitor (Amersham Pharmacia Biotech, Piscataway, NJ) and were harvested with a cell scraper. Cell debris was removed by centrifuging the cell lysate at 13,000 rpm for 10 minutes at 4°C. Protein concentration was determined using the Bio-Rad Protein Assay (Bio-Rad, Hercules, CA) and 20 µg of proteins were loaded on 10% SDS-PAGE gels and separated by gel electrophoresis. Proteins were then transferred to a Polyvinylidene Fluoride (PVDF) membrane (Bio-Rad) and blocked overnight with 5% non-fat milk in Tris buffered saline with 0.1% Tween 20. Proteins were blotted with antibodies against FOXM1 (1:4000, Abcam, Cambridge, UK) and beta-actin (1:5000, Sigma, St. Louis, MO). Detection of the primary antibody was accomplished by using HRP-conjugated anti-mouse IgG (1:10000, GE Healthcare, UK). Protein bands were detected with Super-

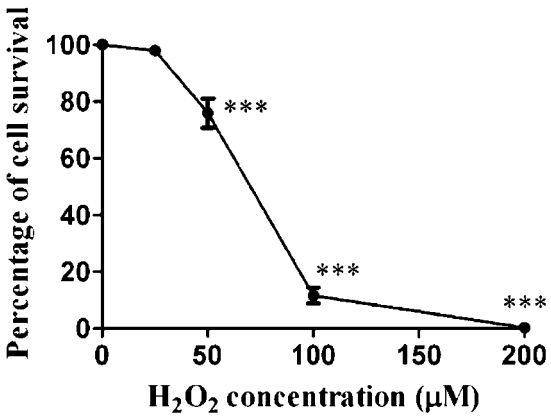

Figure 1. Effect of H_2O_2 treatment on the viability of MCF-7 breast cancer cells. Cells were exposed to 0–200 μM H_2O_2 and cell viability was evaluated by the CellTiter 96® AQueous Non-Radioactive Cell Proliferation Assay. Percentage cell survival was determined by the ratio of optical density (OD) of test sample/OD of control × 100%. The data shown are means ± SEM of three separate experiments in triplicate. *** $P < 0.001$ compared to control.

Signal West Pico Chemiluminescent Substrate (Pierce, Rockford, IL). Protein bands were analyzed and quantified by densitometry.

Statistical Analysis. All data are expressed as mean ± SEM. A Student's *t* test was performed to determine the statistical significance of the cell viability assay. A One Way Analysis of Variance (ANOVA) followed by a Tukey post test was performed for the rest of the data analysis. Statistical analysis was conducted using the GraphPad Prism software (San Diego, CA). $P < 0.05$ was regarded as statistically significant.

Results

H_2O_2 Induces Cytotoxicity in a Dose-Dependent Manner. In order to examine the oxidative damage effects of H_2O_2 treatment in MCF-7 cells, cells were exposed to different concentrations of H_2O_2 for 24 hours. It was noted that H_2O_2 exposure lead to cell death in a concentration-dependent manner. There was no statistically significant difference when MCF-7 cells were treated with a concentration less than 50 μM H_2O_2 when compared to the control group (Fig. 1). However, a significant reduction in cell numbers was seen when MCF-7 cells were treated with concentrations equal to and higher than 50 μM H_2O_2. There was more than 80% reduction of cell numbers when cells were treated with 100 μM H_2O_2 (Figs. 1 and 2). At a concentration of 200 μM H_2O_2, no viable cells were observed. The IC_{50} H_2O_2 was determined as 68.4 μM and IC_{10} H_2O_2 was 34.6 μM, respectively.

H_2O_2 Causes Cell Cycle Arrest and Apoptosis. To test the effect of H_2O_2 on the different phases of cell cycle, MCF-7 cells were treated with IC_{10} H_2O_2 for 24 hours and analysis of the cell cycle profiles were performed. As shown in Figure 3, 34.6 μM H_2O_2 induced G1/S cell cycle arrest with more than 80% accumulation of cells in the G1 phase. Approximately 6% of cells were in sub-G1 (apoptotic) phase after 24 hours treatment, which was significantly higher than in untreated cells. The presence of apoptosis in H_2O_2 exposed cells was verified by DAPI staining, which showed nuclear condensation and chromatin margination (Fig. 4).

H_2O_2 Generates Lipid Peroxidative Stress. The formation of MDA-TBA (malondialdehyde-thiobarbituric acid) adducts is indicative of oxidative stress. To correlate cell viability with oxidative stress, a TBARS assay was performed. There was significantly higher MDA-TBA formation in H_2O_2-treated MCF-7 cells as compared to untreated cells (Fig. 5). A higher MDA-TBA formation in MCF-7 cells was also observed in cells exposed to IC_{50} H_2O_2 as compared with IC_{10} H_2O_2.

H_2O_2 Induces Differential Regulation of Oxidative Stress Related Genes. We also examined the expression of 84 oxidative stress related genes in MCF-7 cells when exposed to IC_{10} H_2O_2 using the Human Oxidative Stress and Antioxidant Defense RT^2 Profiler PCR Array. There were five genes which were found to be differentially regulated with H_2O_2 treatment (Table 1). There was up-regulation of the *Cytoglobin (CYGB)* gene and down-regulation of *Forkhead box M1 (FOXM1), NADPH oxidase* (*NOX5), Nudix (nucleoside diphosphate linked moiety X)-type motif 1 (NUDT1)* and *Selenoprotein*

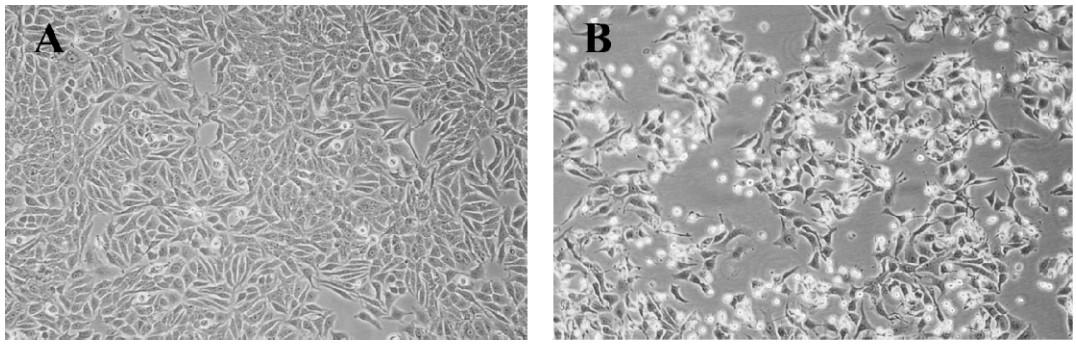

Figure 2. Effect of treatment with 100 μM H_2O_2 for 24 hours on the phenotype of MCF-7 cells as shown by phase contrast microscopy. (A) Untreated cells were confluent and closely adhered to the substratum. (B) H_2O_2-treated cells were unhealthy and many cells rounded up and detached. Magnification: ×10.

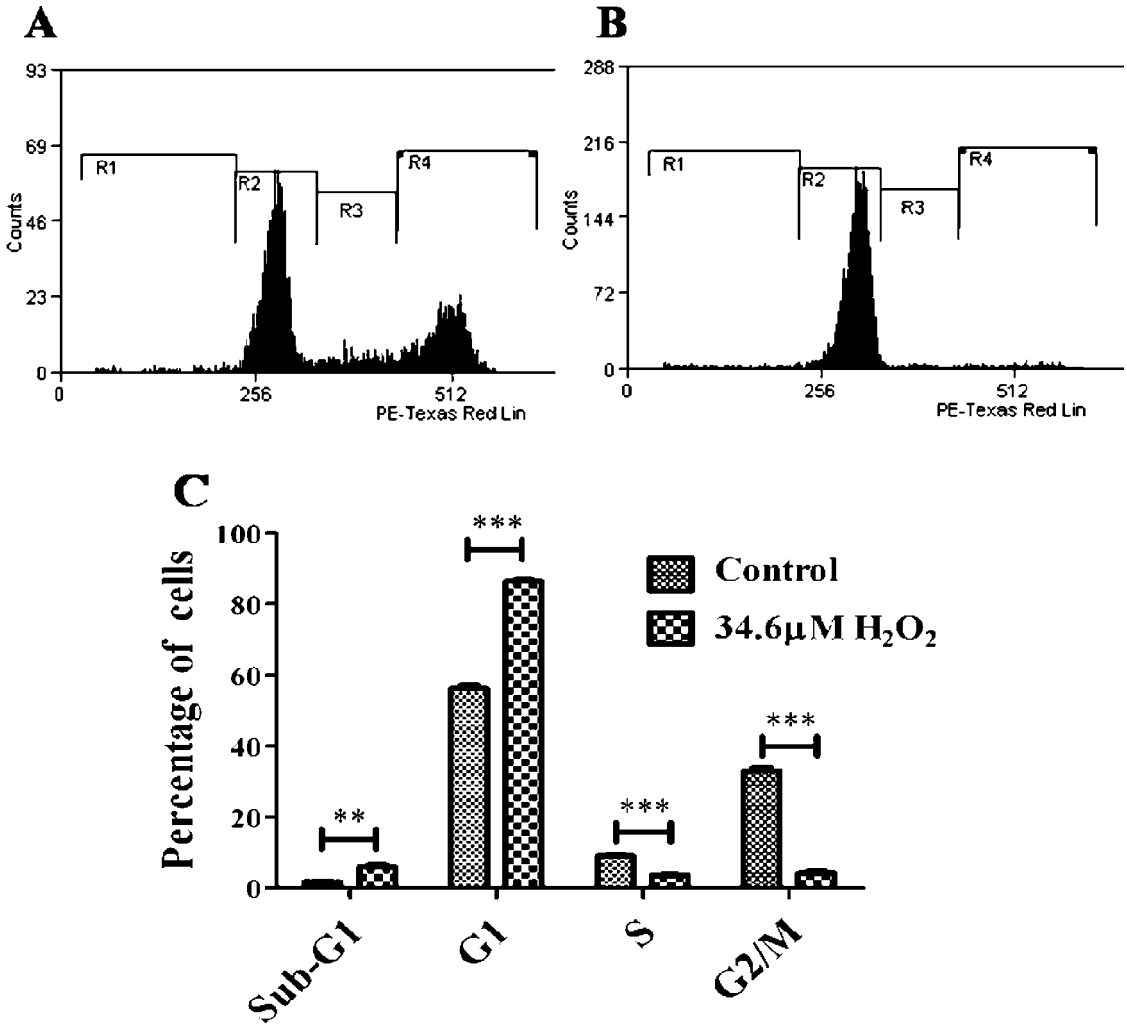

Figure 3. Effect of H_2O_2 treatment on the cell cycle in MCF-7. Cells were treated with 34.6 μM of H_2O_2 and were harvested for cell cycle analysis. The cell cycle distribution was determined using propidium iodide staining and analyzed with flow cytometry. (A) Representative cell cycle profile for untreated cells. (B) Representative cell cycle profile for 34.6 μM H_2O_2-treated cells. R1-sub-G1 phase, R2-G1 phase, R3-S phase, R4-G2/M phase. (C) Bar chart showing the percentage of cells in different phases of cell cycle for untreated and H_2O_2 treated cells. The experiments were in triplicates. Data presented as means ± SEM. ** $P < 0.01$; *** $P < 0.001$.

P1 (SEPP1) genes. The other 79 oxidative stress related genes that were analyzed and found to be unaffected by H_2O_2 treatment are shown in Table 2.

H_2O_2 Consistently Decreases *FOXM1* mRNA and FOXM1 Protein Expression at Different Concentrations. As FOXM1 has been associated with cancer progression and was the most differentially down-regulated gene in this study, expression of the *FOXM1* gene in MCF-7 cells exposed to increasing concentrations of H_2O_2 was examined. H_2O_2-treated cells showed a consistent reduction of *FOXM1* gene expression (Fig. 6A) concomitant with down-regulation of the FOXM1 protein (Fig. 6B).

Table 1. Differentially Regulated Oxidative Stress Related Genes in MCF-7 Breast Cancer Cells with H_2O_2 Treatment

Gene	Description	GenBank accession no.	Fold difference[a]	*P* value
CYGB	Cytoglobin	NM_134268	7.19	0.0033
FOXM1	Forkhead box M1	NM_021953	−4.29	0.0454
NOX5	NADPH oxidase, EF-hand calcium binding domain 5	NM_024505	−2.76	0.0372
NUDT1	Nudix (nucleoside diphosphate linked moiety X)-type motif 1	NM_002452	−1.80	0.0002
SEPP1	Selenoprotein P, plasma, 1	NM_005410	−3.04	0.0418

[a] Positive values indicate up-regulation of the gene while negative values indicate down-regulation of the gene.

Table 2. Oxidative Stress Related Genes in MCF-7 Breast Cancer Cells Not Affected by H_2O_2 Treatment

Gene	Description	Fold change	*P* value	Gene	Description	Fold change	*P* value
ALB	Albumin	2.72	0.5381	MTL5	Metallothionein-like 5, testis-specific (tesmin)	−1.54	0.5676
ALOX12	Arachidonate 12-lipoxygenase	2.94	0.5189	NCF1	Neutrophil cytosolic factor 1 (chronic granulomatous disease, autosomal 1)	1.98	0.6503
ANGPTL7	Angiopoietin-like 7	1.76	0.6740	NCF2	Neutrophil cytosolic factor 2 (65 kDa, chronic granulomatous disease, autosomal 2)	5.35	0.1463
AOX1	Aldehyde oxidase 1	−1.39	0.4431	NME5	Non-metastatic cells 5, protein expressed in (nucleoside-diphosphate kinase)	1.59	0.3575
APOE	Apolipoprotein E	2.62	0.2409	NOS2A	Nitric oxide synthase 2A (inducible, hepatocytes)	3.70	0.3548
ATOX1	ATX1 antioxidant protein1 homolog (yeast)	1.07	0.7682	OXR1	Oxidation resistance 1	−1.17	0.4113
BNIP3	BCL2/adenovirus E1B 19 kDa interacting protein 3	1.66	0.3547	OXSR1	Oxidative-stress responsive 1	1.03	0.9336
CAT	Catalase	−1.41	0.5533	PDLIM1	PDZ and LIM domain 1 (elfin)	1.51	0.1028
CCL5	Chemokine (C-C motif) ligand 5	1.27	0.6179	PIP3-E	Phosphoinositide-binding protein	−1.46	0.7281
CCS	Copper chaperone for superoxide dismutase	−1.01	0.9577	PNKP	Polynucleotide kinase 3′-phosphatase	−1.23	0.2994
CSDE1	Cold shock domain containing E1 RNA-binding	1.26	0.4604	PRDX1	Peroxiredoxin 1	2.11	0.1602
CYBA	Cytochrome b-245, alpha polypeptide	1.06	0.9702	PRDX2	Peroxiredoxin 2	−1.25	0.4889
DGKK	Diacylglycerol kinase, kappa	1.98	0.2135	PRDX3	Peroxiredoxin 3	−1.60	0.5346
DHCR24	24-dehydrocholesterol reductase	−1.35	0.3404	PRDX4	Peroxiredoxin 4	−1.09	0.3046
DUOX1	Dual oxidase 1	1.45	0.7143	PRDX5	Peroxiredoxin 5	1.21	0.1891
DUOX2	Dual oxidase 2	1.98	0.2135	PRDX6	Peroxiredoxin 6	−1.06	0.7532
DUSP1	Dual specificity phosphatase 1	3.69	0.2973	PREX1	Phosphatidylinositol 3,4,5-trisphosphate-dependent RAC exchanger 1	1.02	0.9468
EPHX2	Epoxide hydrolase 2, cytoplasmic	1.44	0.5905	PRG3	Proteoglycan 3	1.69	0.5292
EPX	Eosinophil peroxidase	3.03	0.4548	PRNP	Prion protein (p27–30) (Creutzfeldt-Jakob disease, Gerstmann-Strausler-Scheinker syndrome, fatal familial insomnia)	2.19	0.1558
GLRX2	Glutaredoxin 2	1.17	0.4525	PTGS1	Prostaglandin-endoperoxide synthase 1 (prostaglandin G/H synthase and cyclooxygenase)	2.20	0.1569
GPR156	G protein-coupled receptor 156	2.00	0.6107	PTGS2	Prostaglandin-endoperoxide synthase 2 (prostaglandin G/H synthase and cyclooxygenase)	1.15	0.8123
GPX1	Glutathione peroxidase 1	1.54	0.5536	PXDN	Peroxidasin homolog (Drosophila)	1.25	0.5150
GPX2	Glutathione peroxidase 2 (gastrointestinal)	6.19	0.1156	PXDNL	Peroxidasin homolog (Drosophila)-like	1.31	0.7314
GPX3	Glutathione peroxidase 3 (plasma)	1.80	0.1111	RNF7	Ring finger protein 7	1.28	0.2932
GPX4	Glutathione peroxidase 4 (phospholipid hydroperoxidase)	1.23	0.4146	SCARA3	Scavenger receptor class A, member 3	−1.24	0.2245

Table 2. Continued.

Gene	Description	Fold change	*P* value	Gene	Description	Fold change	*P* value
GPX5	Glutathione peroxidase 5 (epididymal androgen-related protein)	1.69	0.6266	SELS	Selenoprotein S	1.12	0.7999
GPX6	Glutathione peroxidase 6 (olfactory)	1.42	0.6202	SFTPD	Surfactant, pulmonary-associated protein D	−1.03	0.9033
GPX7	Glutathione peroxidase 7	1.98	0.2135	SGK2	Serum/glucocorticoid regulated kinase 2	5.82	0.4034
GSR	Glutathione reductase	2.53	0.1813	SIRT2	Sirtuin (silent mating type information regulation 2 homolog) 2 (S. cerevisiae)	1.34	0.1699
GSS	Glutathione synthetase	−1.01	0.9552	SOD1	Superoxide dismutase 1, soluble (amyotrophic lateral sclerosis 1, adult)	1.34	0.2330
GSTZ1	Glutathione transferase zeta 1 (maleylacetoacetate isomerase)	−1.32	0.5391	SOD2	Superoxide dismutase 2, mitochondrial	−1.09	0.7248
GTF2I	General transcription factor II	−1.30	0.5094	SOD3	Superoxide dismutase 3, extracellular	1.39	0.1853
KRT1	Keratin 1 (epidermolytic hyperkeratosis)	4.09	0.3210	SRXN1	Sulfiredoxin 1 homolog (S. cerevisiae)	4.06	0.4400
LPO	Lactoperoxidase	6.95	0.3500	STK25	Serine/threonine kinase 25 (STE20 homolog, yeast)	1.14	0.5015
MBL2	Mannose-binding lectin (protein C) 2, soluble (opsonic defect)	1.98	0.2135	TPO	Thyroid peroxidase	−1.14	0.6926
MGST3	Microsomal glutathione S-transferase 3	−1.28	0.5985	TTN	Titin	8.24	0.2134
MPO	Myeloperoxidase	4.49	0.3107	TXNDC2	Thioredoxin domain containing 2 (spermatozoa)	3.73	0.3273
MPV17	MpV17 mitochondrial inner membrane protein	−1.02	0.9460	TXNRD1	Thioredoxin reductase 1	7.20	0.2024
MSRA	Methionine sulfoxide reductase A	−1.25	0.7155	TXNRD2	Thioredoxin reductase 2	1.06	0.5241
MT3	Metallothionein 3	3.50	0.3433				

Discussion

Oxidative stress is often defined as an imbalance between ROS level and antioxidant activity in cells which lead to cellular damage (13, 14). When MCF-7 cells were treated with H_2O_2, cell viability was severely compromised with increase in H_2O_2 concentration. There was also an associated impairment of cell cycle progression and induction of apoptosis. This is in concert with the finding that high concentrations of H_2O_2 can cause cells to undergo cell cycle arrest, apoptosis and/or necrosis (15). In addition, a significant increase in lipid peroxidation in H_2O_2 treated cells was detected using the TBARS assay.

Superarray analysis of oxidative stress related genes in cells exposed to H_2O_2 revealed that five out of 84 genes showed statistically significant differences in fold changes, namely *CYGB, FOXM1, NOX5, NUDT1* and *SEPP1*. CYGB, a recently discovered intracellular respiratory globin protein was found to be expressed in the nucleus and the cytoplasm of many types of human tissue and cells (16). In this assay, the *CYGB gene* was up-regulated by 7 folds when treated with H_2O_2, suggesting that this stress-responsive hemoprotein might be a general adaptive response under adverse conditions.

With regard to the down-regulated genes, *NOX5* encodes a novel superoxide-producing NADPH oxidase which is regulated by GTPase Rac 1 and although its physiological function is poorly understood, it has been found to be the primary source of ROS in mature malignant B cells through regulation of SHP-1 tyrosine phosphate activity (17). NUDT1 is important in hydrolyzing oxidized triphosphate 8-oxodGTP to the monophosphate 8-oxodGMP, thereby preventing the mutagenic consequences from oxidation of cellular DNA, RNA and their precursor nucleotides (18, 19). SEPP1 is an antioxidant and selenium transporter which contains multiple selenocysteine residues and binds to about 50% of the total selenium in plasma (20). Studies have shown that the FOXM1 signaling pathway is often deregulated in human malignancies by overexpression of FOXM1 in human hepatocellular carcinoma (21), intrahepatic cholangiocarcinomas (22), infiltrating ductal

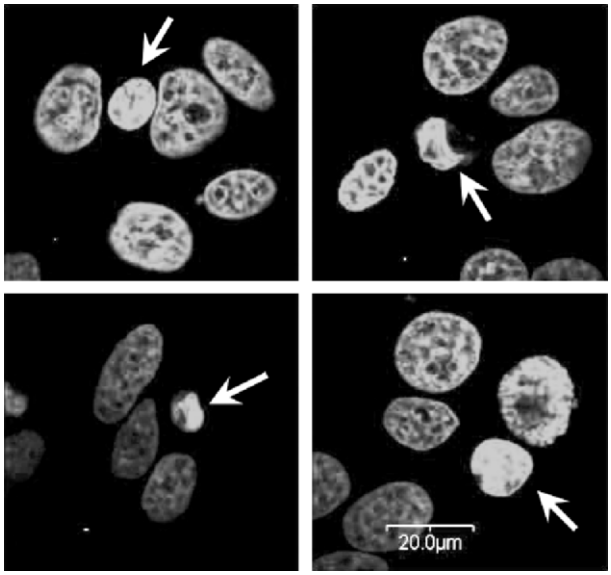

Figure 4. Effect of H_2O_2 on apoptosis in MCF-7 cells. Cells were treated with 34.6 μM H_2O_2 for 24 hours and stained with DAPI dye. Morphological characteristics associated with apoptosis were present when viewed under confocal microscopy. Typical apoptotic cells H_2O_2 are indicated by arrows. Bar = 20 μm.

breast carcinoma (23), glioblastoma (24), basal cell carcinoma (25), non-small cell lung cancers (26), cervical squamous cell carcinoma (27) and in many other human derived tumors (28). *FOXM1* is a proliferation-specific gene which plays important roles in the cellular developmental pathway ranging from cell differentiation to transformation. The FOXM1 protein is a key cell cycle regulator of both the G1 to S phase transition and mitosis progression (29, 30). There is ample evidence that its expression is associated with stimulation of proliferation in numerous tumor derived

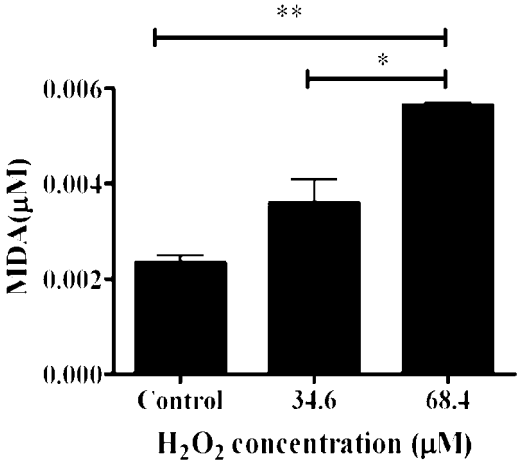

Figure 5. Effect of H_2O_2 treatment on lipid peroxidative stress in MCF-7 breast cancer cells. Cells were exposed to H_2O_2 for 24 hours and the TBARS assay was used to determine the formation of lipid peroxidative products. Data are expressed as means ± SEM. * $P < 0.05$; ** $P < 0.01$.

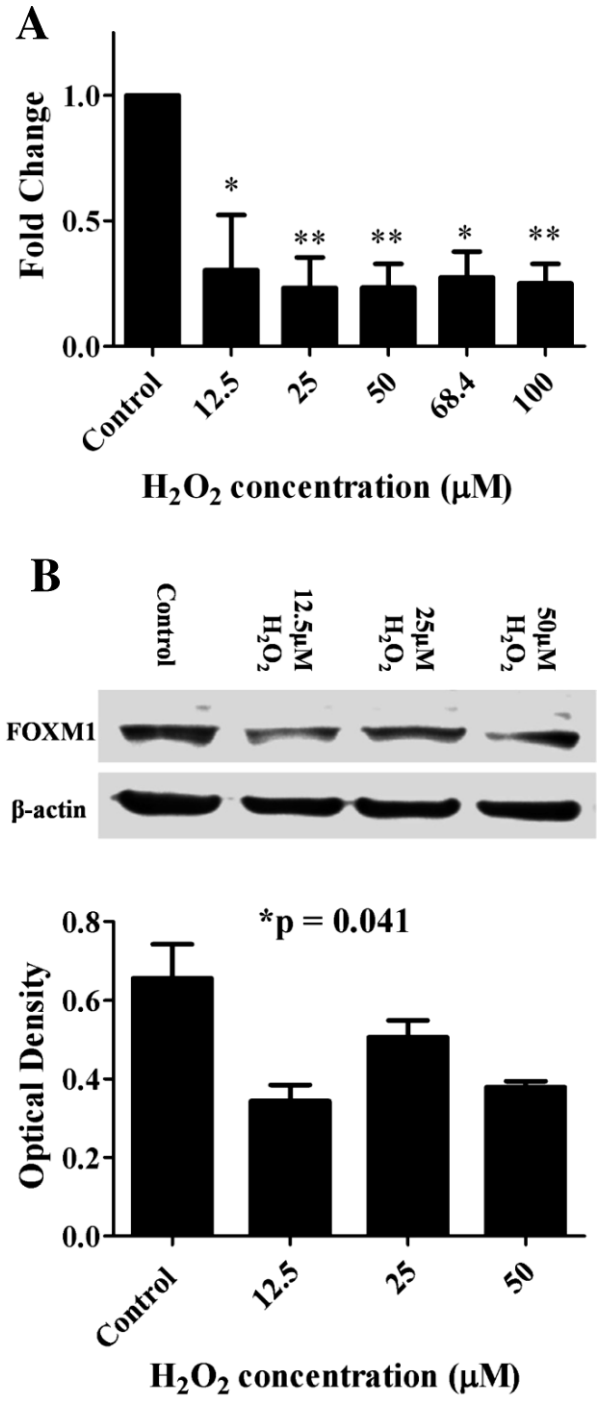

Figure 6. Effect of H_2O_2 treatment on FOXM1 expression. (A) MCF-7 cells were incubated in the different concentration of H_2O_2 for 24 hours. After extraction of RNA, 0.5 μg of total RNA for each sample was converted to cDNA and analyzed by quantitative real time RT-PCR. The difference in the Ct value of *FOXM1* and the *G3PDH* gene was calculated to determine the level of expression of *FOXM1*. Experiments were done in triplicates. Data presented as means ± SEM. * $P < 0.05$; ** $P < 0.01$ as compared with control value. (B)Cells were treated with four concentrations of H_2O_2 for 24 hours and proteins were extracted from cell lysates after 48 hours. Western blot analysis was performed using the FOXM1 antibody with beta actin as the housekeeping control. Upper panel shows a representative blot and lower panel, a bar chart of the quantitation of the protein bands by densitometry. Experiments were done in duplicates. Data presented as means ± SEM.

cell lines (31–35). Studies have shown that FOXM1 regulates transcription of several cell cycle genes including cyclin B, Cdc25A, Cdc25B, cyclin D1, $p21^{Cip1}$, $p27^{Kip1}$, Aurora B kinase and Polo-like kinase (36–40). Decrease in the expression of *FoxM1* is associated with reduced expression of cell cycle regulatory genes involved in the progression of the cell through the S, G2 and M phases (37, 41, 42). Moreover, it has also been previously reported in mouse fibroblasts that H_2O_2 could induce a transient multi-phase cell cycle arrest through modulation of cyclin D and $p21^{Cip1}$ expression (43). Hence, FOXM1 could be a potential cancer therapeutic target for inhibiting cell proliferation.

In summary, the viabilities of MCF-7 cells were severely compromised with increasing H_2O_2 concentration. There was also associated G1/S phase arrest and increased apoptosis. The generation of oxidative stress induced concomitant and differential regulation of oxidative stress associated genes, *CYGB, FOXM1, NOX5, NUDT1* and *SEPP1*. Modulation of the expression of these genes, in particular, *FOXM1* may stifle cancer development, inhibit progression and enhance the efficacy of chemotherapeutic drugs which exert their cytotoxic effects by oxidative stress.

1. Ames BN, Shigenaga MK, Gold LS. DNA lesions, inducible DNA repair, and cell division: three key factors in mutagenesis and carcinogenesis. Environ Health Perspect 101 Suppl 5:35–44, 1993.
2. Cerutti PA. Oxy-radicals and cancer. Lancet 344:862–863, 1994.
3. Nagai T, Yamada K, Kim HC, Kim YS, Noda Y, Imura A, Nabeshima Y, Nabeshima T. Cognition impairment in the genetic model of aging klotho gene mutant mice: a role of oxidative stress. FASEB J 17:50–52, 2003.
4. Casadesus G, Smith MA, Zhu X, Aliev G, Cash AD, Honda K, Petersen RB, Perry G. Alzheimer disease: evidence for a central pathogenic role of iron-mediated reactive oxygen species. J Alzheimers Dis 6:165–169, 2004.
5. Veech GA, Dennis J, Keeney PM, Fall CP, Swerdlow RH, Parker WD Jr, Bennett JP Jr. Disrupted mitochondrial electron transport function increases expression of anti-apoptotic bcl-2 and bcl-X(L) proteins in SH-SY5Y neuroblastoma and in Parkinson disease hybrid cells through oxidative stress. J Neurosci Res 61:693–700, 2000.
6. Harrison D, Griendling KK, Landmesser U, Hornig B, Drexler H. Role of oxidative stress in atherosclerosis. Am J Cardiol 91:7A–11A, 2003.
7. Storz P. Reactive oxygen species in tumor progression. Front Biosci 10: 1881–1896, 2005.
8. Droge W. Free radicals in the physiological control of cell function. Physiol Rev 282:47–95, 2002.
9. Ohno Y, Gallin JI. Diffusion of extracellular hydrogen peroxide into intracellular compartments of human neutrophils. Studies utilizing the inactivation of myeloperoxidase by hydrogen peroxide and azide. J Biol Chem 260:8438–8446, 1985.
10. Schubert J, Wilmer JW. Does hydrogen peroxide exist "free" in biological systems? Free Radic Biol Med 11:545–555, 1991.
11. Valko M, Rhodes CJ, Moncol J, Izakovic M, Mazur M. Free radicals, metals and antioxidants in oxidative stress-induced cancer. Chem Biol Interact 160:1–40, 2006.
12. Valko M, Leibfritz D, Moncol J, Cronin MT, Mazur M, Telser J. Free radicals and antioxidants in normal physiological functions and human disease. Int J Biochem Cell Biol 39:44–84, 2007.
13. Cross CE, Halliwell B, Borish ET, Pryor WA, Ames BN, Saul RL, McCord JM, Harman D. Oxygen radicals and human disease. Ann Intern Med 107:526–545, 1987.
14. Halliwell B, Gutteridge JM, Cross CE. Free radicals, antioxidants, and human disease: where are we now? J Lab Clin Med 119:598–620, 1992.
15. Davies KJ. The broad spectrum of responses to oxidants in proliferating cells: a new paradigm for oxidative stress. IUBMB Life 48:41–47, 1999.
16. Burmester T, Ebner B, Weich B, Hankeln T. Cytoglobin: a novel globin type ubiquitously expressed in vertebrate tissues. Mol Biol Evol 19:416–421, 2002.
17. Geiszt M. NADPH oxidases: new kids on the block. Cardiovasc Res 71:289–299, 2006.
18. Chow E, Thirlwell C, Macrae F, Lipton L. Colorectal cancer and inherited mutations in base-excision repair. Lancet Oncol 5:600–606, 2004.
19. Kang D, Nishida J, Iyama A, Nakabeppu Y, Furuichi M, Fujiwara T, Sekiguchi M, Takeshige K. Intracellular localization of 8-oxo-dGTPase in human cells, with special reference to the role of the enzyme in mitochondria. J Biol Chem 270:14659–14665, 1995.
20. Moghadaszadeh B, Beggs AH. Selenoproteins and their impact on human health through diverse physiological pathways. Physiology (Bethesda) 21:307–315, 2006.
21. Lee JS, Chu IS, Heo J, Calvisi DF, Sun Z, Roskams T, Durnez A, Demetris AJ, Thorgeirsson SS. Classification and prediction of survival in hepatocellular carcinoma by gene expression profiling. Hepatology 40:667–676, 2004.
22. Obama K, Ura K, Li M, Katagiri T, Tsunoda T, Nomura A, Satoh S, Nakamura Y, Furukawa Y. Genome-wide analysis of gene expression in human intrahepatic cholangiocarcinoma. Hepatology 41:1339–1348, 2005.
23. Wonsey DR, Follettie MT. Loss of the forkhead transcription factor FoxM1 causes centrosome amplification and mitotic catastrophe. Cancer Res 65:5181–5189, 2005.
24. van den Boom J, Wolter M, Kuick R, Misek DE, Youkilis AS, Wechsler DS, Sommer C, Reifenberger G, Hanash SM. Characterization of gene expression profiles associated with glioma progression using oligonucleotide-based microarray analysis and real-time reverse transcription-polymerase chain reaction. Am J Pathol 163:1033–1043, 2003.
25. Teh MT, Wong ST, Neill GW, Ghali LR, Philpott MP, Quinn AG. FOXM1 is a downstream target of Gli1 in basal cell carcinomas. Cancer Res 62:4773–4780, 2002.
26. Kim IM, Ackerson T, Ramakrishna S, Tretiakova M, Wang IC, Kalin TV, Major ML, Gusarova GA, Yoder HM, Costa RH, Kalinichenko VV. The Forkhead Box m1 transcription factor stimulates the proliferation of tumor cells during development of lung cancer. Cancer Res 66:2153–2161, 2006.
27. Chan DW, Yu SY, Chiu PM, Yao KM, Liu VW, Cheung AN, Ngan HY. Over-expression of FOXM1 transcription factor is associated with cervical cancer progression and pathogenesis. J Pathol 215:245–252, 2008.
28. 28 Pilarsky C, Wenzig M, Specht T, Saeger HD, Grutzmann R. Identification and validation of commonly overexpressed genes in solid tumors by comparison of microarray data. Neoplasia 6:744–750, 2004.
29. Krupczak-Hollis K, Wang X, Kalinichenko VV, Gusarova GA, Wang IC, Dennewitz MB, Yoder HM, Kiyokawa H, Kaestner KH, Costa RH. The mouse Forkhead Box m1 transcription factor is essential for hepatoblast mitosis and development of intrahepatic bile ducts and vessels during liver morphogenesis. Dev Biol 276:74–88, 2004.
30. Costa RH, Kalinichenko VV, Major ML, Raychaudhuri P. New and unexpected: forkhead meets ARF. Curr Opin Genet Dev 15:42–48, 2005.
31. Korver W, Roose J, Clevers H. The winged-helix transcription factor

Trident is expressed in cycling cells. Nucleic Acids Res 25:1715–1719, 1997.

32. Ye H, Kelly TF, Samadani U, Lim L, Rubio S, Overdier DG, Roebuck KA, Costa RH. Hepatocyte nuclear factor 3/fork head homolog 11 is expressed in proliferating epithelial and mesenchymal cells of embryonic and adult tissues. Mol Cell Biol 117:1626–1641, 1997.
33. Kalin TV, Wang IC, Ackerson TJ, Major ML, Detrisac CJ, Kalinichenko VV, Lyubimov A, Costa RH. Increased levels of the FoxM1 transcription factor accelerate development and progression of prostate carcinomas in both TRAMP and LADY transgenic mice. Cancer Res 66:1712–1720, 2006.
34. Korver W, Roose J, Wilson A, Clevers H. The winged-helix transcription factor Trident is expressed in actively dividing lymphocytes. Immunobiology 198:157–161, 1997.
35. Liu M, Dai B, Kang SH, Ban K, Huang FJ, Lang FF, Aldape KD, Xie TX, Pelloski CE, Xie K, Sawaya R, Huang S. FoxM1B is overexpressed in human glioblastomas and critically regulates the tumorigenicity of glioma cells. Cancer Res 66:3593–3602, 2006.
36. Leung TW, Lin SS, Tsang AC, Tong CS, Ching JC, Leung WY, Gimlich R, Wong GG, Yao KM. Over-expression of FoxM1 stimulates cyclin B1 expression. FEBS Lett 507:59–66, 2001.
37. Wang X, Kiyokawa H, Dennewitz MB, Costa RH. The Forkhead Box m1b transcription factor is essential for hepatocyte DNA replication and mitosis during mouse liver regeneration. Proc Natl Acad Sci U S A 99: 16881–16886, 2002.
38. Ye H, Holterman AX, Yoo KW, Franks RR, Costa RH. Premature expression of the winged helix transcription factor HFH-11B in regenerating mouse liver accelerates hepatocyte entry into S phase. Mol Cell Biol 19:8570–8580, 1999.
39. Wang X, Hung NJ, Costa RH. Earlier expression of the transcription factor HFH-11B diminishes induction of p21(CIP1/WAF1) levels and accelerates mouse hepatocyte entry into S-phase following carbon tetrachloride liver injury. Hepatology 33:1404–1414, 2001.
40. Wang X, Krupczak-Hollis K, Tan Y, Dennewitz MB, Adami GR, Costa RH. Increased hepatic Forkhead Box M1B (FoxM1B) levels in old-aged mice stimulated liver regeneration through diminished $p27^{Kip1}$ protein levels and increased Cdc25B expression. J Biol Chem 277: 44310–44316, 2002.
41. Kalinichenko VV, Major ML, Wang X, Petrovic V, Kuechle J, Yoder HM, Dennewitz MB, Shin B, Datta A, Raychaudhuri P, Costa RH. Foxm1b transcription factor is essential for development of hepatocellular carcinomas and is negatively regulated by the p19ARF tumor suppressor. Genes Dev 18:830–850, 2004.
42. Kim IM, Ramakrishna S, Gusarova GA, Yoder HM, Costa RH, Kalinichenko VV. The forkhead box m1 transcription factor is essential for embryonic development of pulmonary vasculature. J Biol Chem 280:22278–22286, 2005.
43. Barnouin K, Dubuisson ML, Child ES, Fernandez de MS, Glassford J, Medema RH, Mann DJ, Lam EW. H_2O_2 induces a transient multi-phase cell cycle arrest in mouse fibroblasts through modulating cyclin D and $p21^{Cip1}$ expression. J Biol Chem 277:13761–13770, 2002.